Electronic Supplementary Information

for:

Selective and stoichiometric incorporation of ATP by self-assembling amyloid fibrils.

by

Robert Dec,[1,2] Wojciech Puławski,[2] and Wojciech Dzwolak[1*,2]

[1]Faculty of Chemistry, Biological and Chemical Research Centre, University of Warsaw, 1 Pasteur Street, 02-093 Warsaw, Poland. [2]Institute of High Pressure Physics, Polish Academy of Sciences, 29/37 Sokołowska Street, 01-142 Warsaw, Poland

[*] Corresponding author: Dzwolak; Phone: +48 22 552 6567; Fax: +48 22 552 4029 ; E-mail: wdzwolak@chem.uw.edu.pl

Contents

A. Materials

The amino acid sequence of the $ACC_{1-13}K_8$ peptide (GIVEQCAASVCSLKKKKKKKK) consists of the first 13 N-terminal residues of bovine insulin's A-chain extended at the C-end by additional 8 lysine residues. In addition, cysteine residue at the position 7, which in the parent insulin molecule is involved in the interchain disulfide bond (Cys7A-Cys7B), has been substituted with alanine. The peptide retains the parent insulin's original intrachain Cys6-Cys11 disulfide bond. $ACC_{1-13}K_8$ peptide, as well as ACC_{1-13} and K_8 fragments, all without N- or C-terminal modifications, were custom-synthesized by Pepscan (Lelystad, The Netherlands) at a high purity exceeding 97 %, and were delivered by the manufacturer as trifluoroacetic acid (TFA) salts. ATP (adenosine 5'-triphosphate disodium salt), ADP (adenosine 5'-diphosphate sodium salt) and AMP (adenosine 5'-diphosphate free acid) and all other non-peptidic chemicals were from MilliporeSigma (Sigma-Aldrich).

B. Samples

Due to the high lysine content stock TFA salts of $ACC_{1-13}K_8$ and K_8 dissolve readily in water. Therefore the typical procedure of preparation of a peptide-nucleotide sample consisted in rapid mixing of aqueous stock solutions of $ACC_{1-13}K_8$ or K_8 (pH 6.5) with a portion of stock solution of ATP (ADP, AMP, or sodium phosphate), pH pre-adjusted to 6.5, to obtain desired peptide : nucleotide molar ratios. Typically, molar peptide concentrations in plate-reader-monitored kinetic experiments were kept constant at 0.15 mM while nucleotide concentrations varied (Figs. 1b and 2a). Highly hydrophobic and agglomerated ACC_{1-13} peptide required a more elaborate and earlier described solubilization protocol consisting in initial dispersion of solid peptide sample in 8M guanidine hydrochloride (GdnHCl) solution, pH 9.0 [S1]. Aggregation of ACC_{1-13} (as carried out in the control experiment reported in Fig. 2b) was triggered by rapid dilution of its concentrated stock solution in 8 M GdnHCl with an excess of appropriately acidified water / ATP solution. As a result, the aggregation of ACC_{1-13} took place in the presence of residual GdnHCl (at 1.33 M concentration).

C. Methods

C.1. Fibrillization kinetics (Thioflavin T fluorescence assay)

ThT-fluorescence measurements ($\lambda_{ex.}$ 440 nm / $\lambda_{em.}$ 485 nm) of peptide/ATP co-aggregation kinetics were carried out on a CLARIOstar® plate reader from BMG LABTECH (Offenburg, Germany) using 96-well black microplates. Typically, each well was filled with a 150 µL portion of freshly mixed peptide/nucleotide liquid sample containing an addition of thioflavin T (ThT) at the 20 µM concentration. Measurements were carried out at 37 ^{o}C and moderate agitation (300 rpm) for at least 24 hours, as specified. Each kinetic trace was calculated as an average from three independently collected trajectories (error bars correspond to standard deviations). Afterward, aggregate samples were collected from the plate washed

with portions of water in order to remove excess of unbound ATP and salts. Eluted pellets were subjected to atomic force microscopy (AFM), and FT-IR (Fourier transform infrared) spectroscopic measurements.

C.2. Atomic force microscopy (AFM)

A small portion of $ACC_{1\text{-}13}K_8$-ATP aggregate suspension collected from the microplate after the kinetic experiment was initially washed several times with water. Subsequently, pellet suspension was further diluted with water until the aggregate concentration reached the range of approximately 0.1 mg/mL. A small droplet (10 µl) of this suspension was swiftly deposited onto freshly cleaved mica and left to dry overnight. AFM tapping-mode measurements were carried out using a Nanoscope III atomic force microscope from Veeco Instruments (Plainview, NY, USA) and TAP300-Al sensors (res. frequency 300 kHz) from BudgetSensors (Sofia, Bulgaria).

C.3. Attenuated total reflectance (ATR) FT-IR measurements

Centrifuged samples of aggregates collected from the microplate at the end of the kinetic experiment were washed several times with equal portions water in order to remove unbound ATP. Suspensions of fibrils were deposited and allowed to dry up on diamond surface of single-reflection diamond ATR accessory of Nicolet iS50 FT-IR spectrometer from Thermo Fisher Scientific (Waltham, MA, USA) equipped with a DTGS detector. Typically, for a single ATR FT-IR spectrum 32 interferograms of 2 cm^{-1} resolution were co-added. Due to ambiguity in determining real values of refractive indexes of peptide-ATP amyloid aggregates only uncorrected ATR FT-IR data is shown. Spectral data processing was limited to subtracting water vapor spectrum and adjusting 2 point baseline using GRAMS software (Thermo Fisher Scientific).

C.4. Circular dichroism (CD) measurements

For the CD measurements presented in Fig. 3a the peptide-nucleotide co-aggregation in freshly mixed solution containing 0.15 mM $ACC_{1\text{-}13}K_8$, 0.45 mM ATP, 20 µM ThT, pH 6.5 was monitored using the plate reader which enabled tracking aggregation progress by monitoring ThT emission (left inset in Fig. 3a). Small portions of the mixed solution were collected from the plate after the indicated periods of time and subsequently diluted 20 times with water before being placed in a 10 mm quartz cuvette. CD measurements followed. For the CD measurements of the monomeric species shown in the right inset of Fig. 3a, 7.5 µM $ACC_{1\text{-}13}K_8$ and 100 µM ATP, both in water pH 6.5, and a 10 mm cuvette were used. All CD spectra corrected for the buffer signal were acquired at room temperature by accumulation of 5 independent spectra (at 200 nm/s scanning rate) on a J-815 S spectropolarimeter from Jasco Corp. (Tokyo, Japan).

C.5. Structural visualization

Molecular dynamics (MD) simulations were carried out using AMBER 18 GPU implementation [S2-S3]. FF15ipq forcefield ([S4]) was used for the peptide and SPCe model for water. ATP molecules were modelled with parameters as described earlier [S5]. $ACC_{1\text{-}13}K_8$ monomer model was prepared as an extended polypeptide chain with ideal β-sheet

dihedrals (-135 degs / 135 degs) constrained by disulfide bond between CYS6 and CYS11. Flat $ACC_{1\text{-}13}K_8$ monomers were docked to each other using the procedure described previously [S6] assuming an in-register parallel β-sheet architecture. In total, 20 layers of $ACC_{1\text{-}13}K_8$ were stacked in order to create the amyloid core architecture to which 40 ATP molecules, 40 Na^+ and 40 Cl^- ions were added. The system was solvated within a 95 x 75 x 124 $Å^3$ water box and then minimized, gradually heated to 300 K and finally equilibrated during a 50 ns period using NPT ensemble with 2 fs timestep. The production phase, three independent runs for 500 ns, was conducted in the NVT ensemble. In the course of ATP-peptide docking simulation, positional restraints were applied to all protein's C_α carbon atoms with respect to their initial positions with spring constant of 1.0 kcal/mol/ $Å^2$.

In order to investigate impact of ATP presence on the structural stability of pre-assembled $ACC_{1\text{-}13}K_8$ fibril, the constrains on C_α carbon atoms were removed (the 500 ns-long stability simulations shown in Fig. S3). Additionally, as a control simulation, another system was built with an identical $ACC_{1\text{-}13}K_8$ fibril but depleted of ATP molecules (charge neutrality was maintained through the adjustment of Na^+ / Cl^- concentration). The fibril was immersed in a 68 x 81 x 126 $Å^3$ SPCe water box and neutralized with Na^+ / Cl^- ions. The same heating protocol was applied for the production phase. All constraints applied to C_α carbon atoms were removed.

D. Time-lapse AFM

Co-aggregation of $ACC_{1\text{-}13}K_8$ and ATP was carried out using typical conditions (0.15 mM peptide concentration, a molar excess of ATP vs. peptide (1 ATP per 2 lysine residues), pH 6.5, 37 °C, and was monitored with the ThT fluorescence assay using a plate reader. The progress of aggregation is shown in the top left panel of Fig. S1. At selected intervals small volumes of the mixed solution were collected and appropriately diluted with water (see the C.2 section) and subsequently transferred onto freshly cleaved mica. After 24 hours, tapping mode AFM measurements of thus obtained dry films followed.

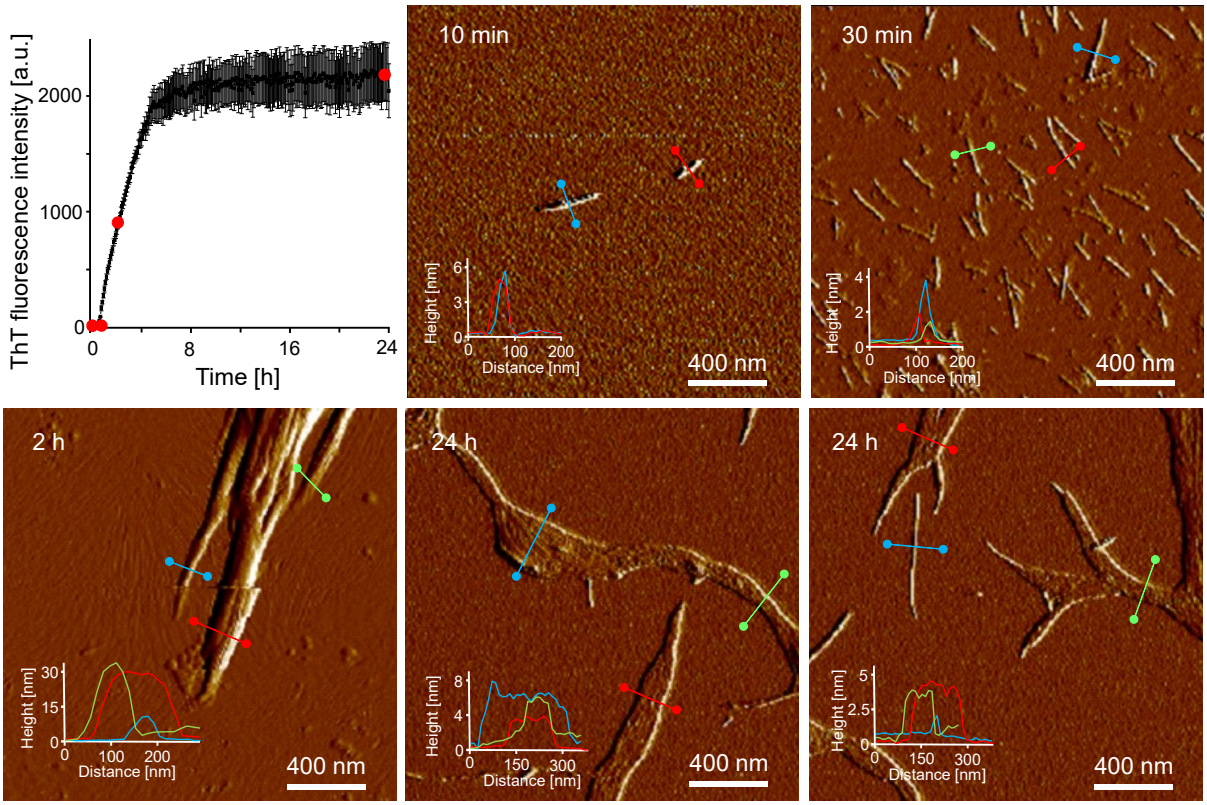

Figure S1. Time-lapse AFM amplitude images of $ACC_{1\text{-}13}K_8$ and ATP co-aggregation. Samples were collected at various stages of ThT-fluorescence-monitored process, as indicated in the top left panel (red points). Superimposed are cross-sections of selected specimen.

E. *In silico* analysis of clustering of adenine moieties in $ACC_{1\text{-}13}K_8$-ATP amyloid

The MD-based simulations were carried out under the conditions specified in section C.5. While the amyloid scaffold was pre-assembled in the fashion of parallel in-register β-sheet, and the peptide backbones were constrained accordingly throughout the simulation, the side chains, ATP molecules, and added counter-ions were unconstrained. The following Fig.

S2 presents consecutive snapshots selected at different time intervals from a 500 ns long simulation. For the sake of clarity, only peptide backbone and adenine moieties are presented.

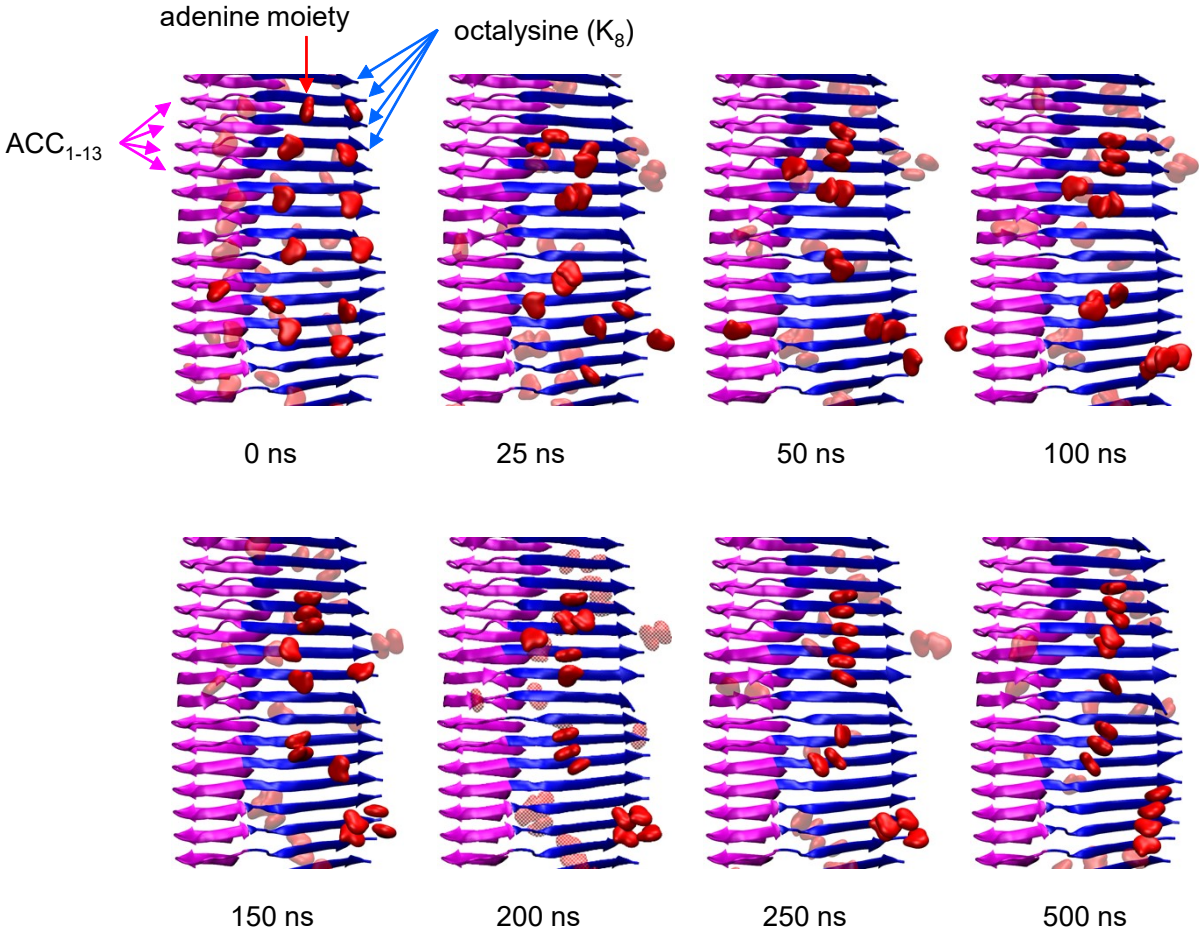

Figure S2. MD snapshots of the spontaneous stacking of adenine moieties upon docking of ATP onto $ACC_{1-13}K_8$ fibril surface. Color code: ACC_{1-13} segment, magenta; K_8 segment, blue; ATP's adenine moiety, red bean. Amino acid side chains and polyphosphate / ribose moieties are purposefully omitted from these images for the sake of clarity.

F. *In silico* probe of $ACC_{1-13}K_8$ amyloid stability in the presence and absence of ATP

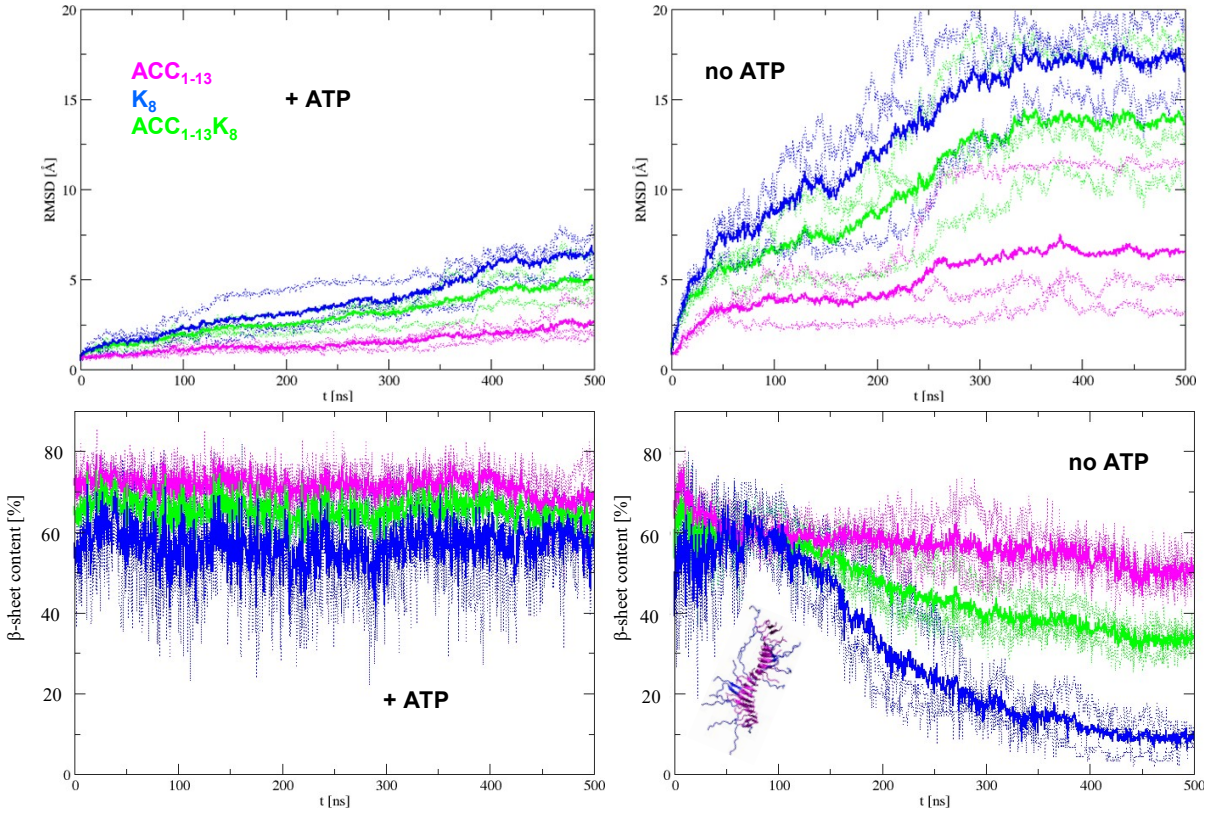

Figure S3. MD-based investigation of the conformational stability of pre-assembled $ACC_{1-13}K_8$ fibril in the presence (left panels) and absence (right panels) of ATP (see section C.5 for details). The trajectories were obtained by plotting RMSD (top panels) and transient β-sheet content (bottom panels) as functions of time. These parameters were calculated for the whole peptide (green), as well as for its separate portions corresponding to ACC_{1-13} (magenta) and K_8 (blue) segments. Binding of ATP results in structural stabilization and preservation of β-sheet content. The ATP depletion has a more pronounced destabilizing effect on the K_8 fragment than on the amyloid core ACC_{1-13} segment: see the snapshot of a partly disassembled fibril after 500 ns of simulation shown in the inset in the right bottom panel.

G. References

S1. R. Dec, M. Koliński, & W. Dzwolak “Beyond amino acid sequence: disulfide bonds and the origins of the extreme amyloidogenic properties of insulin's H - fragment” ***FEBS J.*** 2019, *286*, 3194-3205.

S2. D.A. Case, I.Y. Ben-Shalom, S.R. Brozell, D.S. Cerutti, T.E. Cheatham, III, V.W.D. Cruzeiro, T.A. Darden,R.E. Duke, D. Ghoreishi, M.K. Gilson, H. Gohlke, A.W. Goetz, D. Greene,R Harris, N. Homeyer, Y. Huang,S. Izadi, A. Kovalenko, T. Kurtzman, T.S. Lee, S. LeGrand, P. Li, C. Lin, J. Liu, T. Luchko, R. Luo, D.J.Mermelstein, K.M. Merz, Y. Miao, G. Monard, C. Nguyen, H. Nguyen, I. Omelyan, A. Onufriev, F. Pan, R.Qi, D.R. Roe, A. Roitberg, C. Sagui, S. Schott-Verdugo, J. Shen, C.L. Simmerling, J. Smith, R. Salomon-Ferrer, J. Swails, R.C. Walker, J. Wang, H. Wei, R.M. Wolf, X. Wu, L. Xiao, D.M. York & P.A. Kollman (2018), AMBER 2018, University of California, San Francisco

S3. R. Salomon-Ferrer, A.W. Götz, D. Poole, S. Le Grand & R.C. Walker “Routine microsecond molecular dynamics simulations with AMBER on GPUs. 2. Explicit solvent particle mesh Ewald” ***J. Chem. Theory Comput.*** 2013, *9*, 3878-3888.

S4. K.T. Debiec, D.S. Cerutti, L.R. Baker, A.M. Gronenborn, D.A. Case, & L.T. Chong “Further along the road less traveled: AMBER ff15ipq, an original protein force field built on a self-consistent physical model” ***J. Chem. Theory Comput.*** 2016, *12*, 3926-3947.

S5. K.L. Meagher, L.T. Redman, & H.A. Carlson “Development of polyphosphate parameters for use with the AMBER force field. ***J. Comput. Chem.*** 2003, *24*, 1016-1025.

S6. M. Wacławska, M. Guza, G. Ścibisz, M. Fortunka, R. Dec, W. Puławski, & W. Dzwolak, W. „Reversible Freeze-Induced β-Sheet-to-Disorder Transition in Aggregated Homopolypeptide System” ***J. Phys. Chem. B*** 2019, *123*, 9080-9086.